

Distribution and Characteristics of the Occluding Junctions in a Monolayer of a Cell Line (MDCK) Derived from Canine Kidney

Carlos A. Rabito, Ruy Tchao, John Valentich, and Joseph Leighton

Cancer Bioassay Laboratory, Department of Pathology,
The Medical College of Pennsylvania, Philadelphia, Pennsylvania 19129

Received 14 April 1978; revised 21 July 1978

Summary. On solid substrates MDCK, a cell line derived from normal dog kidney, forms a confluent monolayer that is studded with "blisters". Previous studies with this cell line suggest that these hemicysts develop as a result of active fluid accumulation between cell sheet and substratum. One factor that may determine when and how hemicysts appear only in localized sites is the interruption of occluding junctions in nonhemicyst areas. To study this possibility, we compared the permeability characteristics of the occluding junctions in hemicysts and in an uninterrupted monolayer of MDCK grown on a permeable support of collagen-coated nucleopore filter. The spontaneous electrical potential differences were small, without statistical differences between them. Relative ionic permeability coefficients were evaluated from the voltage deflections to imposed salt gradients or to a single ion substitution across both structures. The results showed that the relative permeability ratios for Na^+ , K^+ , choline⁺, and Cl^- were the same in hemicysts and the uninterrupted monolayer. These and other results indicate that the junctional complex encircling the apical surface of a sheet of MDCK cells can provide an effective permeability barrier constituting a true occluding junction with the same properties in hemicyst and nonhemicyst areas.

In 1969 Leighton *et al.* [10] described the occurrence of fluid-filled blister-like hemicysts in cultures of MDCK, a cell line derived from a normal dog kidney, which grows as a papillary adenocarcinoma in the chick embryo and in nude mice. Since then hemicysts have been reported in other normal and neoplastic cell cultures [8, 13, 17, 20-23]. In each instance, the cells cultured were from transporting epithelia.

Time lapse cinematographic study has demonstrated that the hemicysts in MDCK monolayers were dynamic structures [11], and that ouabain, an inhibitor of active solute transport, abolished hemicyst formation [1]. Mg^{++} and Mn^{++} had the same effect, while dbc-AMP, papaverine, and Ca^{++} enhanced hemicyst formation [24]. Ouabain-sensitive ATPase activity has been demonstrated by biochemical measurement [1]. All of these findings suggest that hemicyst formation in MDCK

monolayers is associated with active transport of solutes accompanied by water.

Growing MDCK cells on a permeable support, such as a membrane filter [14] or on collagen coated discs of a fine mesh nylon cloth [5], and then mounting the flat sheet between Lucite chambers presents new opportunities to study the properties of this epithelial layer in an accurate way. MDCK cells cultured on a freely permeable membrane filter generated an electrical potential difference with the apical surface negative and water flux in absence of a chemical gradient [14]. This monolayer also shows an alkali-cation selectivity pattern $K > Na > Rb > Cs > Li$ [5] similar to that found in other biological membranes [9].

One important aspect of hemicyst formation is that these structures occupy only a small fraction of the total area of the monolayer. This raises the following question. If we grow the monolayer on a permeable support, mounted later between Lucite chambers to test membrane properties, will these properties correspond to a uniform membrane? As an alternative, are the hemicysts an expression of a group of cells with different transport or permeability properties from the cells in areas without hemicysts?

In this study we attempt to test one aspect of this problem: whether the occluding junctions encircling the apical end of each MDCK cell have the same permeability properties of the monolayer in two different conditions—in the hemicyst itself and in a monolayer grown on a permeable collagen-coated Nucleopore filter. Any difference in these two conditions would be attributed to the presence of nonhemicyst areas as they occur on glass. Growing MDCK cells on collagen-coated Nucleopore filters does not apparently alter their functional properties relative to cells on glass substrata. Although hemicysts do not develop on collagen-coated filters this is solely due to the permeability of the support since hemicysts will form on collagen-coated glass. (C.A. Rabito, *unpublished*).

Materials and Methods

Maintenance and Cultures

MDCK cells were maintained by serial passage in stoppered 32 oz. prescription bottles at 36 °C. The cells were fed with Eagle's minimal essential medium prepared in equal volumes of Earle's and Hanks' balanced salt solution (Microbiological Associates, Bethesda, Md.). The medium was supplemented with 15% calf serum, L-glutamine (2 mM), penicillin (100 units per ml), streptomycin (50 µg per ml), and Fungizone (1 µg/ml). The medium was changed 2 or 3 times a week and the pH of the medium was maintained between 6.6 and 7.4. When cell

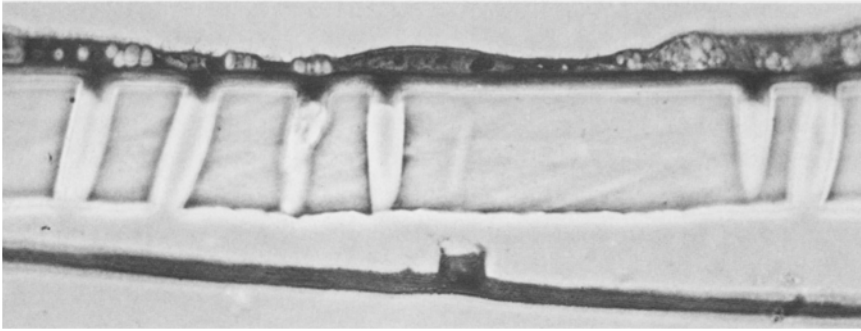


Fig. 1. Thick section cut perpendicular to the collagen coated nucleopore filter (pore size $5\ \mu\text{m}$) and MDCK monolayer. The collagen film (*cf*) covering both faces of the filter prevents direct contact between the MDCK monolayer (*m*) and filter (*n*). Intracellular lipid droplets are seen in some cells of the monolayer. The total thickness of the collagen coated filter is $15\text{--}20\ \mu\text{m}$ (compared with the thickness of the filter = $10\ \mu\text{m}$). Toluidine Blue stain. Phase contrast, $\times 1300$

growth reached saturation density, subcultures were prepared using 0.02% EDTA- 0.05% trypsin (Grand Island, N.Y.).

Preparation of Hemicysts and Monolayer

Cultures for hemicysts and monolayer were prepared in large Leighton tubes containing a sterile standard glass microscope slide. Each tube was inoculated with $5\ \text{ml}$ of cells suspended in medium at approximately 10^6 cells per ml to reach a cell density of 5×10^5 cells cm^{-2} . The cultures were fed every 2 or 3 days with $5\ \text{ml}$ of medium during the 5 days prior to making the electrical measurements.

Monolayers on a permeable support were prepared using a polycarbonate filter membrane with $5\ \mu\text{m}$ pore size and $25\ \text{mm}$ diameter (Nucleopore, Pleasanton, Calif.). To increase cell adhesion to the support and to avoid cells penetrating and occluding the pores, both faces of the filter membrane were covered with a very thin film of 1% collagen dispersion (Ethicon, Somerville, N.J.) and applied to a glass slide. The collagen was precipitated and aggregated into native bundles by ammonia vapor [2] resulting in its adhesion to glass. The collagen-coated membrane was sterilized with a 70% alcohol solution. The total thickness of this trilaminar membrane was 15 to $20\ \mu\text{m}$ (Fig. 1). It was sufficiently transparent for most analyses by transmitted light microscopy. The subsequent procedure before using the monolayer was exactly like that for monolayer on glass support.

Solution

Hanks' solution was used for dilution potential determination. The standard Hanks' solution has the following composition (mM): $136.8\ \text{NaCl}$, $5.63\ \text{KCl}$, $1.26\ \text{CaCl}_2$, $0.49\ \text{MgCl}_2$, $0.45\ \text{MgSO}_4$, $4.16\ \text{NaHCO}_3$, $0.33\ \text{Na}_2\text{HPO}_4$, $0.44\ \text{KH}_2\text{PO}_4$, $5.5\ \text{glucose}$, pH 7.42. Isosmotic dilutions were prepared by mixing different proportions of Hanks' complete solution and Hanks' solution without NaCl, made isosmotic with sucrose. In this way it was possible to obtain Hanks' solution with different concentrations of NaCl, maintaining constant con-

centrations of all other ions. All these solutions were supplemented with 15% calf serum of known electrolyte composition. The final NaCl concentration was calculated taking into account the serum contribution. Biionic potentials were measured by replacing 114 mM NaCl with 114 mM KCl, LiCl, RbCl, CsCl, or choline Cl. All solutions were prepared from reagent grade chemicals. The electrolyte composition was checked using simultaneous multiple analyzer model SMA-6 (Technicon Co., Tarrytown, N.Y.).

Measurement of the Activity Coefficient for Choline Chloride

An apparent activity coefficient for choline chloride was measured with a Ag/AgCl electrode, using as control a NaCl solution corrected for the activity coefficient obtained from Robinson and Stokes [19]. In this way any error in the preparation of the choline chloride solution was included in this apparent activity coefficient.

Light and Electron Microscopy

For light microscopy, the monolayer was fixed in 10% alcoholic formalin solution and stained with hematoxylin and eosin.

For electron microscopy, cultures were fixed for 20 to 30 min, at 4 °C with 2.5% glutaraldehyde in 0.1 M cacodylate buffer (pH 7.4), followed by a wash with the buffer solution and post-fixation for 20 to 30 min at 4 °C with 1% osmium tetroxide in 0.1 M cacodylate buffer. Visualization of membrane structure was significantly enhanced if cultures were stained *en bloc* with 2% aqueous uranyl acetate for 1 hr at 4 °C after osmium fixation. Cultures were dehydrated in graded ethanol, treated with propylene oxide, and embedded in Epon 812. Sections were picked up on collodion-coated copper grids, double stained with uranyl acetate and Reynold's lead acetate, and examined at 60 to 80 kV with a Zeiss EM 10A electron microscope.

Electrical Measurement

Microelectrode Determination

Ling-Gerard type micro-electrodes were pulled from glass Pyrex tubing 1.1 mm OD \times 0.6 mm ID and filled with 2.8 M KCl. The electrical resistance of the electrodes ranged from 30 to 50 M Ω . Electrodes were discarded if the tip potential was greater than ± 5 mV. The mean tip potential was -1.28 ± 0.15 mV. The microelectrodes were connected to a Ag/AgCl electrode, and potentials recorded on an Orion model 701 pH meter used as potentiometer connected to a Grass model 76 polygraph recorder. The electrodes were always prepared the day before making the electrical determinations.

The microscope slides with cell cultures were removed from the culture tubes and placed in a plastic Petric dish containing Hanks' solution. The solution was removed by aspiration and new solution was added with a syringe.

Randomly selected hemicysts were used for the measurement of transepithelial electrical potential. The technique is illustrated in Fig. 2. A microelectrode was inserted into a hemicyst. Success in penetration was checked by visual inspection and by a reversible potential change resulting from a change in the test solution. (Fig. 3.)

Chamber Determinations

The collagen-coated filter with the monolayer was removed from the culture tube and mounted as a flat sheet between two Lucite half chambers with a window area of 3.14 cm². To reduce edge damage, the filter was placed between two silicone rubber rings coated with

METHOD FOR MEASURING DILUTION AND BI-IONIC POTENTIAL ACROSS HEMICYST WALL

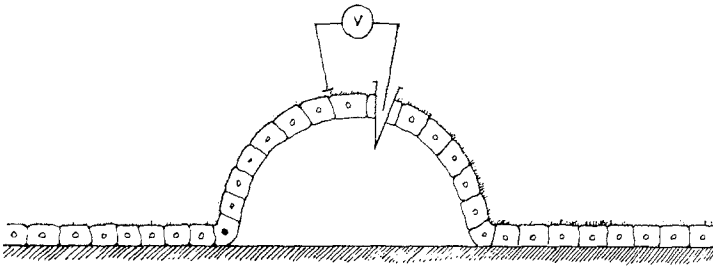


Fig. 2. Method used for measuring electrical potential differences across the hemicyst wall. Success in penetration was assessed by inspection and by reversible alterations in potential produced by changes in the test solution

TRACING FROM A REPRESENTATIVE DILUTION POTENTIAL IN A HEMICYST

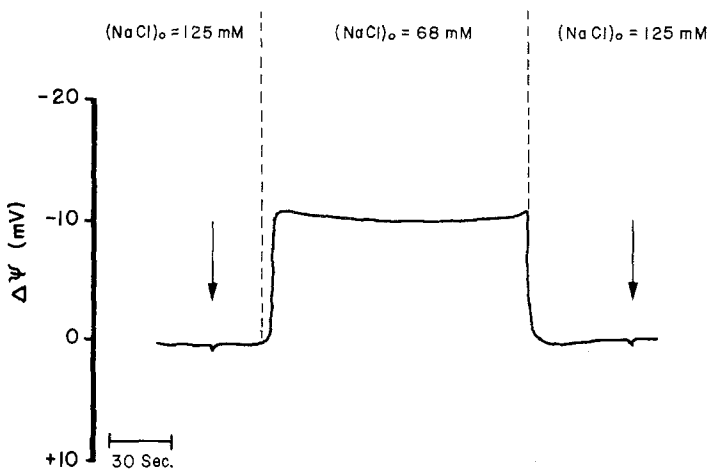


Fig. 3. Tracing illustrating a representative dilution potential across a hemicyst wall. The first arrow indicates penetration of the microelectrode into the hemicyst cavity. The time interval between the two broken vertical lines is when NaCl in the outside bathing solution is partly replaced by sucrose. The arrow to the right indicates withdrawal of the microelectrode from the hemicyst cavity

Dow Corning High Vacuum Silicone Grease as sealant [4]. Each chamber contained 8 ml of solution which was vigorously stirred by a magnetic stirring bar.

Transepithelial potential differences were measured with an Orion model 701 pH meter. The electrodes used were pairs of Ag/AgCl-KCl or calomel electrodes connected to the bathing solutions by bridges of 3.0 M KCl, immobilized by 4% agar at 5 mm from the tissue.



Fig. 4. MDCK cells growing as a monolayer on a collagen coated Nucleopore filter. Note the collagen fibrils (*cf*) with typical periodicity covering the filter (*n*). Microvilli (*mv*) and occluding junctions (*oj*) are seen at the cell surface facing the bulk medium. (*d*) Desmosome. 18,000 \times

The total asymmetry with Hanks' solution in both sides was never more than 0.2 mV. Corrections for differences in electrode potential due to junction potentials were not made. Current was measured with a CSC microammeter model 320 G (The Triplett Corp., Bluffton, Ohio), and was conducted by Ag/AgCl electrodes on opposite sides of the membrane and at the rear of the chamber.

Experimental Protocol

For consistency in nomenclature and because the monolayer is by morphologic criteria an asymmetric epithelial membrane structure, we call the apical side of the monolayer occupied by microvilli "outer part" and the basal side of the monolayer facing the glass substrate or the collagen coated filter "inner part" (Fig. 4).

All experiments were performed at 25 °C. The inside solution was Hanks' complete medium. To obtain the dilution or biionic potentials, changes in the composition were made in the outside solution. For conductance measurements, an outside solution identical in composition to the inside solution was used. The potential difference values ($\Delta\psi$) were obtained every 30 sec until a steady or quasi-steady state was achieved, generally within a fraction of a minute, and maintained for at least several minutes thereafter. After each two measurements of biionic potentials, a 1.00:1.82 NaCl dilution potential was measured.

Calculation of Permeability Ratios

The permeability ratios from measured $\Delta\psi$ were extracted by means of the Goldman-Hodgkin-Katz equation.

$$\Delta\psi = -\frac{RT}{F} \ln \frac{P_{\text{Na}} a_{\text{Na}}^i + P_{\text{K}} a_{\text{K}}^i + P_{\text{Cl}} a_{\text{Cl}}^o}{P_{\text{Na}} a_{\text{Na}}^o + P_{\text{K}} a_{\text{K}}^o + P_{\text{Cl}} a_{\text{Cl}}^i} \quad (1)$$

Where a is the activity of the ionic species shown by the subscript, the superscripts i and o refer to the inside and outside bathing solutions respectively; $\Delta\psi$ is the voltage difference; R , T , and F have their usual meaning; and P are relative permeability coefficients. $P_{\text{Na}}/P_{\text{Cl}}$ was calculated by inserting the measured dilution potential into Eq. (1). The permeability ratios for other cations were calculated by inserting the respective biionic potential and the calculated $P_{\text{Na}}/P_{\text{Cl}}$ into Eq. (1).

Each value in the micropuncture experiments is the mean of 4 determinations in 4 different hemicysts on the same slide. Results are expressed as mean \pm SE (number of observations).

Results*Spontaneous Electrical Potential Difference*

In agreement with the results of Misfeldt *et al.* [14], the $\Delta\psi$, in the absence of ion concentration gradient, was small or negligible. In the hemicysts $\Delta\psi$ was $+1.18 \pm 0.14$ mV [12] and in the monolayer $+0.84 \pm 0.34$ mV [14] without statistical differences between them ($P > 0.2$). The sign of the $\Delta\psi$ corresponds to the inside solution. Both $\Delta\psi$ disappeared when the hemicyst was disrupted by the microelectrode, or when the filter with the monolayer was punctured intentionally.

Relative Ionic Permeability Coefficient

The relative permeability of several ions across the wall of the hemicyst or monolayer was estimated from the extent to which the spontaneous transepithelial potential difference was altered by changes in the composition of the outside solution.

$P_{\text{Na}}/P_{\text{Cl}}$ was estimated from the dilution potential that resulted by imposing different concentration gradients for both sodium and chloride across the epithelium. The tracing from one micropuncture experiment in a hemicyst is displayed in Fig. 3. These results are summarized in Fig. 5, which shows a plot of the voltage change as a function of the log of NaCl activity gradient. There was a significant correlation between $\Delta\psi$ and the

LIQUID JUNCTION POTENTIAL IN MDCK HEMICYSTS

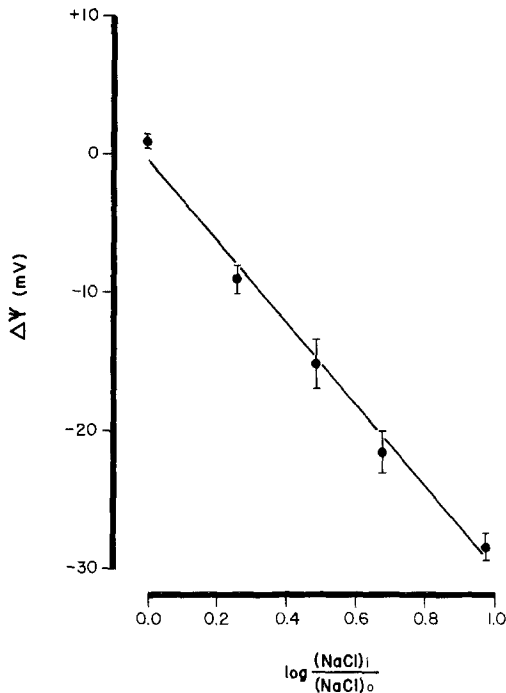


Fig. 5. Relationship between the magnitude of the dilution potential across a hemicyst wall and the logarithm of the imposed NaCl activity gradient. The points represent the mean potential of 12 observations \pm SE for each of the 5 NaCl test solutions. Parentheses are used to express NaCl activity instead of concentration. The line was drawn according to the regression equation shown in the text

log of the activity gradient ($P < 0.01$), which is fitted by the following regression equation.

$$\Delta\psi = -0.31 - 31.56 \log \frac{a_{\text{NaCl}}^i}{a_{\text{NaCl}}^o} \quad (2)$$

$$r = 0.9925.$$

If we use the approach described by Boulpaep *et al.* [3] to calculate the $P_{\text{Na}}/P_{\text{Cl}}$ ratio with the regression slope of this equation, we obtain a value of 3.39 for the hemicyst.

In order to compare the permeability properties of a monolayer with those of a hemicyst, the same type of experiments were repeated using monolayers grown on a collagen coated filter and then placed between two Lucite chambers. $P_{\text{Na}}/P_{\text{Cl}}$ for these membranes was estimated in the same way as for hemicysts, from the dilution potentials that result by

**LIQUID JUNCTION POTENTIAL IN COLLAGEN-COATED
NUCLEOPORE FILTER WITH OR WITHOUT MDCK CELLS**

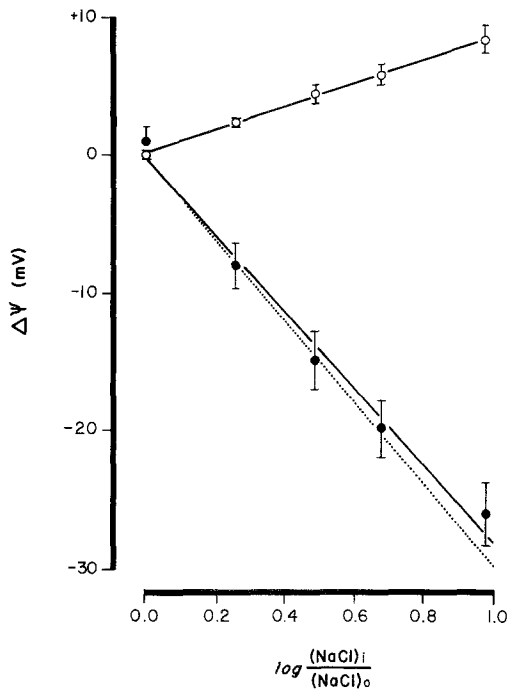


Fig. 6. Relationship between the magnitude of the dilution potential across a collagen coated Nucleopore filter (open circles) and a collagen coated Nucleopore filter covered with a monolayer of MDCK cells (filled circles) and the logarithm of the imposed NaCl activity gradient. The points represent the mean potential of 14 observations \pm se for each of the 5 NaCl test solutions. Lines were drawn using the method of least squares. The broken line is a reproduction of the curve in Fig. 5 drawn here to facilitate comparison between the two types of preparation

imposing different NaCl activity gradients across the epithelium. Figure 6 shows a plot of the voltage change across a monolayer as a function of the log NaCl activity gradient. As before, there was a significant correlation ($P < 0.01$) between $\Delta\psi$ and the log of the activity gradient. From the slope we obtain a $P_{\text{Na}}/P_{\text{Cl}}$ ratio of 3.03. This value is very close to the $P_{\text{Na}}/P_{\text{Cl}}$ value that we obtained in hemicysts; there was no statistical difference ($P < 0.5$) between the regression slopes. The dotted line in Fig. 6 is a copy of the line in Fig. 5 and was drawn to facilitate the comparison.

The equation previously used to calculate the numerical values of $P_{\text{Na}}/P_{\text{Cl}}$ ratios from dilution potential measurements neglected the contribution of any other ion to the observed potential change. However,

Table 1. Permeability ratios of hemicyst and monolayer of MDCK cells

Preparation	P_{Na}/P_{Cl}	P_K/P_{Cl}	P_{Ch}/P_{Cl}
Hemicyst	4.45 ± 0.43 (12) $P < 0.9$	6.24 ± 0.21 (10) $P < 0.9$	< 0.04 (9)
Monolayer	4.35 ± 0.54 (14)	6.15 ± 0.17 (9)	< 0.04 (12)

in spite of the good correlation between $\Delta\psi$ and the log of the NaCl activity gradients, we can observe in Figs. 5 and 6 (filled circles) that the slope between each experimental point shows a tendency to decrease when the NaCl activity gradient across the membrane is increased. The difference is clearer, though still not significant, if we compare the slope between the first two and the last two experimental values. This could mean that when we decreased the outside NaCl activity to increase the NaCl activity gradients across the membrane, the participation of the other ions was increased in our measurements giving us an underestimate of P_{Na}/P_{Cl} value. Because of this and in order to obtain a more real value, we used the Goldman-Hodgkin-Katz equation to obtain the permeability ratios from our measurements of dilution or biionic potentials. The P_{Na}/P_{Cl} ratios calculated in this form were 4.45 ± 0.43 [12] for hemicysts and 4.35 ± 0.54 [14] for the monolayer (Table 1). There was no statistical difference between them ($P > 0.5$).

The P_{Na}/P_{Cl} ratio obtained in the monolayer could be modified by the presence of another barrier: The collagen-coated filter membrane. To study its permeability characteristics and its influence on P_{Na}/P_{Cl} ratio, collagen coated filters without cells were placed between two Lucite chambers and dilution potentials studied as before. Figure 6 (open circles) show that there was also a significant correlation ($P < 0.01$) between $\Delta\psi$ and the log of the NaCl activity gradients. The sign of the potential deflections showed qualitatively a greater permeability for Cl^- than for Na^+ . This is expected in a membrane in which Na^+ and Cl^- have the same mobilities as in free water. The P_{Na}/P_{Cl} ratio calculated from the dilution potentials was 0.686. This is very close to 0.626, the ratio between the mobilities of Na^+ and Cl^- in water. Furthermore, the electrical resistance of the collagen-coated filter was $34.3 \pm 0.87 \Omega \cdot cm^2$ [8], which is very similar to $34.5 \Omega \cdot cm^2$, the electrical resistance of the solution alone.

To obtain the electrical resistance of the monolayer, and since series resistance including solution between the voltage-sensing electrodes was in the same order ($34.3 \Omega \cdot cm^2$), correction was made for a voltage drop

in the adjacent solutions. After this correction the electrical resistance for the monolayer was $173.3 \pm 10.4 \Omega \cdot \text{cm}^2$ [14].

As an extension of these results, Table 1 shows the relative permeability coefficient for two other cations, K^+ and choline⁺. Similar to the results for Na^+ , there was no statistical difference in the relative permeability coefficient for these ions between hemicyst and monolayer. In addition, we observed that membrane permeability for choline was at least one hundred times less than that for Na^+ in both preparations. The biionic potential for choline was $-23.7 \pm 0.96 \text{ mV}$ [9] for hemicysts and $-24.5 \pm 0.86 \text{ mV}$ [12] for the monolayer.

Discussion

$\Delta\psi$ in the absence of a chemical gradient was small and similar in both hemicysts and monolayers. Our studies provide no evidence for the mechanism responsible for the origin of this small $\Delta\psi$.

Morphological polarity, the presence of occluding junctions [14], and the reversible ouabain inhibition of hemicyst formation [1] constitute acceptable evidence that the hemicyst is an epithelium engaged in active transport. In addition, the small spontaneous $\Delta\psi$ and the practical absence of solute gradients across the hemicyst wall (*see* Table 2) means that it is an epithelium with a leaky junction. Similar characteristics are also found in the monolayer. Although at present we do not know the effect of ouabain on the monolayer, all other studies suggest that the monolayer is very similar to the hemicyst in all its properties.

Examination of occluding junctions with freeze-fracture technique has revealed, in cultures of cells dissociated from normal pre-lactating mouse mammary glands or from spontaneous adenocarcinomas, that the occluding junction has the same structure in both hemicyst and non-hemicyst areas [18]. Claude and Goodenough [6] correlated the trans-epithelial permeability of a given epithelium with the structure of its occluding junctions; we can conclude from these results [6, 18] that the occluding junctions at both levels have the same permeability properties. However, from the wide variety of epithelia studied with the freeze-fracture technique, it is clear now that there are important exceptions to the proposed correlation of permeability and occluding junction structure [12–15].

Since the occluding junction is the main pathway for passive ion permeation across the leaky epithelium [7], it is possible by studying the

Table 2. Sodium and potassium concentration of hemicyst fluid and medium in cell culture of MDCK

	Na ⁺ (mM)	K ⁺ (mM)
Hemicyst fluid ^a	149.9 ± 2.49 (9)	7.03 ± 0.28 (9)
Tissue culture medium	145.6 ± 6.22 (9)	6.66 ± 0.94 (9)

^a Samples of fluid from 10 or more hemicysts on the same microscope slide were obtained with a siliconized glass pipette connected through polyethylene tubing to a 1-ml syringe and pooled. Analyses were performed by flame photometry on samples from 9 different cultures.

passive permeability of this epithelium to know the permeability properties of its occluding junction. In this study we have compared the properties of occluding junctions in two different structures, hemicysts and monolayers grown on a permeable support.

NaCl activity gradients across the hemicyst wall were calculated by assuming that the electrolyte concentration inside the hemicyst was the same as that of the culture medium. This assumption was supported by an intercept very close to zero in Eq. (2) and by the virtual absence of Na⁺ and K⁺ gradient between the hemicyst content and the culture media (Table 2).

The P_{Na}/P_{Cl} ratio obtained from the dilution potentials in hemicysts was very similar to that obtained in the monolayer, indicating that the relative permeabilities for Na⁺ and for Cl⁻ are the same in the occluding junctions of both structures. The P_{Na}/P_{Cl} value for the monolayer is about 2.5 times higher than the value reported by Misfeldt *et al.* [14] for MDCK cells grown on a Millipore filter. This difference could be due to the detachment of MDCK cell from the millipore filter during the electrical determinations produced by the stirring of the solution and the low adhesiveness of the cell to the substratum. This possibility is supported by the low resistance value they obtained ($83.7 \Omega \cdot \text{cm}^2$), about half of the value ($173.3 \Omega \cdot \text{cm}^2$) we obtained and by our finding that there is a rapid decline of the resistance during the electrical measurements when Millipore was used as a permeable substratum. Cereijido *et al.* [5] reported a value of electrical resistance similar to Misfeldt's results. However, their value for the P_{Na}/P_{Cl} ratio was about two times higher than ours. One explanation of this difference between our results and that of Cereijido's may be the undulating surface supporting the cells used in their study. This may contribute to an underestimation of the surface area. In our system, cells are supported on a flat sheet where we can determine the surface area precisely. These are not the only differences between Cerei-

Table 3. Relative ionic permeability derived from the dilution and biionic potential in MDCK monolayer

Cation	Dilution potential	Biionic potential	P_{X^+}/P_{Cl^-}	P_{X^+}/P_{K^+}
K ⁺		+ 3.68 ± 0.15 (12)	6.15	1.00
Na ⁺	- 8.14 ± 0.44 (14)		4.35	0.70
Li ⁺		- 3.59 ± 0.26 (14)	3.20	0.52
Rb ⁺		- 4.95 ± 0.29 (14)	3.00	0.49
Cs ⁺		- 9.28 ± 0.47 (14)	2.15	0.35

jido's and our results. Table 3 demonstrates the existence of a qualitatively different alkali-cation selectivity. The permeability sequence obtained from the dilution and biionic potential was $K > Na > Li > Rb > Cs$. This sequence differs from that obtained by Cereijido *et al.* [5] in which the Li position was ranked at the end of the series. The explanation for all of these discrepancies could be also in the differences between a supposedly similar cell line produced by different management or spontaneous mutations of the MDCK cell. Preliminary results on chromosome analysis (J. Leighton, *unpublished*) strongly suggests that the latter possibility could be the cause of this discrepancy. The MDCK cell line used in our experiments has a higher number of chromosomes than the MDCK cells provided by The American Type Culture Collection, Rockville, Md.

The relative permeability determination by microelectrode technique in hemicysts assumed that the lateral diffusion of ions and water through the interspace between MDCK cells and the glass surface surrounding the hemicyst cavity was practically nil. This assumption is supported by the presence of the hemicysts themselves and by cinematographic time lapse study, which shows that the hemicysts are not static structures. They form and expand continuously, apparently under pressure of accumulating fluid. Finally, the hemicyst bursts and promptly collapses to reform again [1]. A small lateral diffusion is difficult to discard, but at least it is so small that it allows the hemicysts to form up to the point at which they burst. This indicates that cell adhesion to the substratum surrounding the hemicyst is equal or tighter than the occluding junctions between the cells on the hemicyst roof. In this form the permeability study of the wall of the hemicysts by micropuncture technique reflects mainly the properties of the occluding junctions.

The P_{Na}/P_{Cl} ratio obtained in the monolayer could reflect the permeability properties of two in-series barriers, the monolayer and the collagen coated filter membrane underneath the monolayer. The small difference between the P_{Na}/P_{Cl} ratio obtained in the collagen coated

filter alone (0.686) and the ratio between the transport number of Na^+ and Cl^- in water (0.626) is probably due to the effect of the unstirred layer discussed by Moreno *et al.* [16]. The high permeability of this membrane also tends to reduce the activity gradient. This result indicates that the mobilities of these ions through the collagen coated filter were practically the same as in water. This finding is supported by the same value obtained for the electrical resistance in the collagen coated filter as in the solution alone. This means that the collagen coated filter membrane had practically a negligible effect on the relative permeability ratios of the monolayer in the present experimental conditions.

An extension of the $P_{\text{Na}}/P_{\text{Cl}}$ results, the similarity of the relative permeability ratios for two other cations, K^+ and choline⁺ (Table 1), obtained in hemicysts and monolayer confirm that there is no difference between the passive permeability of the occluding junctions in both structures.

Comparison between $P_{\text{Na}}/P_{\text{Cl}}$ and $P_{\text{choline}}/P_{\text{Cl}}$ reveal that the membrane is about one hundred times less permeable to choline than to Na^+ in hemicyst and monolayer. The bionic potential for choline obtained in both conditions was very close to -24.3 mV, the equilibrium potential difference for the other ions. This means that choline is practically impermeable across hemicyst and monolayer. The fact that the $P_{\text{Na}}/P_{\text{Cl}}$ ratios were very different from the ratios of the transport number in free water and that the cationic permeability sequence was different from the measured mobilities sequence in aqueous solution strongly suggests that the junctional complex encircling the outside end of each MDCK cell can provide an effective permeability barrier, constituting a truly occluding junction. The similarity in the permeability ratios between hemicyst and monolayer also showed that there was no difference in their permeability properties and that junctional belts were not interrupted in nonhemicyst areas.

We wish to express our thanks to Dr. David Goldman for review and valuable discussion of this manuscript.

The work was supported in part by Public Health Service International Research Fellowship Number F 05 TW 2345, Research Grant CA 14137 from the National Cancer Institute, and Grant Nos. GM 02008 and RR 05418 from the National Institutes of Health.

References

1. Abaza, N.A., Leighton, J., Schultz, S.G. 1974. Effects of ouabain on the function and structure of a cell Line (MDCK) derived from canine kidney. *In Vitro* **10**:172
2. Bornstein, M.B. 1958. Reconstituted rat-tail collagen used as substrate for tissue cultures on coverslips in maximow slides and roller tubes. *Lab. Invest.* **4**:134

3. Boulpaep, E.L., Seely, J.F. 1971. Electrophysiology of proximal and distal tubules in the autoperfused dog kidney. *Am. J. Physiol.* **221**:1084
4. Canessa, M., Labarca, P., Leaf, A. 1976. Metabolic evidence that serosal sodium does not recycle through the active transepithelial transport pathway of toad bladder. *J. Membrane Biol.* **30**:65
5. Cereijido, M., Robbins, E.S., Dolan, W.J., Rotunno, C.A., Sabatini, D.D. 1978. Polarized monolayers formed by epithelial cells on a permeable and translucent support. *J. Cell Biol.* **77**:853
6. Claude, P., Goodenough, D.A. 1973. Fracture faces of *Zonulae occludentes* from "tight" and "leaky" epithelia. *J. Cell Biol.* **58**:390
7. Diamond, J.M. 1977. Twenty-first Bowditch Lecture. The Epithelial Junction: Bridge, Gates and Fence. *Physiologist* **20**:10
8. Enami, J., Nandi, S., Haslam, S. 1973. Production of three-dimensional structures—"domes"—from dissociate mammary epithelial cells of mice. *In Vitro* **8**:405a
9. Gillary, H.L. 1966. Stimulation of the salt receptor of the blowfly. III. The alkali halides. *J. Gen. Physiol.* **50**:359
10. Leighton, J., Brada, Z., Estes, L.W., Justh, G. 1969. Secretory activity and oncogenicity of a cell line (MDCK) derived from canine kidney. *Science* **163**:472
11. Leighton, J., Estes, L.W., Mansukhani, S., Brada, Z. 1970. A cell line derived from normal dog kidney (MDCK) exhibiting qualities of papillary adenocarcinoma and renal tubular epithelium. *Cancer* **26**:1022
12. Martinez-Palomo, A., Erlig, D. 1975. Structure of tight junctions in epithelia with different permeability. *Proc. Nat. Acad. Sci. USA* **12**:4487
13. McGrath, C.M. 1971. Replication of mammary tumor virus in tumor cell cultures: Dependence on hormone-induced cellular organization. *J. Nat. Cancer Inst.* **47**:455
14. Misfeldt, D.S., Hamamoto, S.T., Pitelka, D.R. 1976. Transepithelial transport in cell culture. *Proc. Nat. Acad. Sci. USA* **73**:1212
15. Mollgard, K., Malinowska, D.H., Saunders, N.R. 1976. Lack of correlation between tight junction morphology and permeability properties in developing choroid plexus. *Nature (London)* **264**:293
16. Moreno, J.H., Diamond, J.M. 1974. Discrimination of monovalent inorganic cations by "tight" junctions of gallbladder epithelium. *J. Membrane Biol.* **15**:277
17. Owens, R.B., Smith, H.S., Hackett, A.J. 1974. Epithelial cell cultures from normal glandular tissue of mice. *J. Nat. Cancer Inst.* **53**:261
18. Pickett, P.B., Pitelka, D.R., Hamamoto, S.T., Misfeldt, D.S. 1975. Occluding junctions and cell behaviour in primary cultures of normal and neoplastic mammary gland cells. *J. Cell Biol.* **66**:316
19. Robinson, R.A., Stokes, R.H. 1970. *Electrolyte Solutions*. Butterworths, London
20. Sherman, M.I. 1975. The culture of cells derived from mouse blastocytes. *Cell* **5**:343
21. Smith, R.E., Ellis, L.E., Hull, R.N. 1974. Light, scanning and transmission electron microscopy of "dome-like" structure in a continuous pig kidney cell strain. *J. Cell Biol.* **63**:322a
22. Soulé, H.D., Vasquez, J., Long, A., Albert, S., Brennan, M. 1973. A human cell line from a pleural effusion derived from a breast carcinoma. *J. Nat. Cancer Inst.* **51**:1409
23. Toyoshima, K., Valentich, J.D., Tchao, R., Leighton, J. 1976. Conditions of cultivations required for the formation of hemicysts *in Vitro* by rat bladder carcinoma R-4909. *Cancer Res.* **36**:2800
24. Valentich, J.D., Tchao, R., Leighton, J. 1976. Functional control of transporting epithelia by cAMP and divalent cations. *J. Cell Biol.* **70**:330a